RESEARCH ARTICLE

WILEY

Gelatin methacryloyl as environment for chondrocytes and cell delivery to superficial cartilage defects

Katja Hölzl[1] | Marian Fürsatz[2,3] [ID] | Hakan Göcerler[4] | Barbara Schädl[3,5,6] |
Sara Žigon-Branc[1] | Marica Markovic[1,6] | Claudia Gahleitner[2] |
Jasper Van Hoorick[7] | Sandra Van Vlierberghe[7] | Anne Kleiner[2] | Stefan Baudis[6,8] |
Andreas Pauschitz[9] | Heinz Redl[3,6] | Aleksandr Ovsianikov[1,6] | Sylvia Nürnberger[2,3,6]

[1]Institute of Materials Science and Technology, 3D Printing and Biofabrication Group, TU Wien, Vienna, Austria

[2]Department of Orthopedics and Trauma-Surgery, Division of Trauma-Surgery, Medical University of Vienna, Vienna, Austria

[3]Ludwig Boltzmann Institute for Traumatology, The Research Center in Cooperation with AUVA, Vienna, Austria

[4]Institute of Engineering Design and Product Development, TU Wien, Vienna, Austria

[5]University Clinic of Dentistry, Medical University of Vienna, Vienna, Austria

[6]Austrian Cluster for Tissue Regeneration, Vienna, Austria

[7]Centre of Macromolecular Chemistry, Polymer Chemistry and Biomaterials Group, Ghent University, Ghent, Belgium

[8]Institute of Applied Synthetic Chemistry, TU Wien, Vienna, Austria

[9]AC2T Research GmbH, Wiener Neustadt, Austria

Correspondence
Sylvia Nürnberger, Department of Orthopedics and Trauma-Surgery, Division of Trauma-Surgery, Medical University of Vienna, Vienna, Austria.
Email: sylvia.nuernberger@meduniwien.ac.at

Abstract

Cartilage damage typically starts at its surface, either due to wear or trauma. Treatment of these superficial defects is important in preventing degradation and osteoarthritis. Biomaterials currently used for deep cartilage defects lack appropriate properties for this application. Therefore, we investigated photo-crosslinked gelatin methacryloyl (gelMA) as a candidate for treatment of surface defects. It allows for liquid application, filling of surface defects and forming a protective layer after UV-crosslinking, thereby keeping therapeutic cells in place. gelMA and photo-initiator lithium phenyl-2,4,6-trimethyl-benzoylphosphinate (Li-TPO) concentration were optimized for application as a carrier to create a favorable environment for human articular chondrocytes (hAC). Primary hAC were used in passages 3 and 5, encapsulated into two different gelMA concentrations (7.5 wt% (soft) and 10 wt% (stiff)) and cultivated for 3 weeks with TGF-β3 (0, 1 and 10 ng/mL). Higher TGF-β3 concentrations induced spherical cell morphology independent of gelMA stiffness, while low TGF-β3 concentrations only induced rounded morphology in stiff gelMA. Gene expression did not vary across gel stiffnesses. As a functional model gelMA was loaded with two different cell types (hAC and/or human adipose-derived stem cells [ASC/TERT1]) and applied to human osteochondral osteoarthritic plugs. GelMA attached to the cartilage, smoothened the surface and retained cells in place. Resistance against shear forces was tested using a tribometer, simulating normal human gait and revealing maintained cell viability. In conclusion gelMA is a versatile, biocompatible material with good bonding capabilities to cartilage matrix, allowing sealing and smoothening of superficial cartilage defects while simultaneously delivering therapeutic cells for tissue regeneration.

1 | INTRODUCTION

Regeneration of articular cartilage has been a major focus of regenerative medicine and tissue engineering over the past decades. Articular cartilage is a load-bearing tissue (Bhosale & Richardson, 2008), and is often damaged due to injury or wear as aging proceeds. It has a limited self-healing capability, as chondrocytes are not able to migrate from their surrounding matrix in sufficient numbers to repair the defect (Akkiraju & Nohe, 2015; Sophia Fox et al., 2009). The isolation from adjacent tissues (e.g., bone marrow, synovial membrane) and lack of vascularization does not allow sufficient ingrowth of regenerative cells (e.g., stem cells) (Zhang et al., 2009).

Deep traumatic defects in an otherwise healthy knee joint have multiple treatment options mainly based on the implantation of cells sometimes supported by scaffold biomaterials (e.g., microfracture, [matrix-associated] autologous chondrocyte implantation) (Brittberg et al., 1994; Enea et al., 2012; Hunziker et al., 2015). The intact surrounding cartilage protects from load and allows stabilization and fixation of the biomaterials. In contrast, damage as a consequence of erosion (e.g., osteoarthritis (OA)) and some traumata result in a defect too shallow to shield the implanted biomaterial from load, thereby preventing the use of scaffold materials routinely used in clinics.

Treatment approaches which rely on injection of cell suspensions (e.g., intra-articular stem cell injection) have shown some improvement in long-term clinical studies in osteoarthritic patients. However, they still lead to incomplete recovery and often late deterioration (Garza et al., 2020; Migliorini et al., 2020; Song et al., 2018). One of the reasons for this sub-optimal outcome might be the lack of cell engraftment, either by not adhering or by not being protected from the mechanical forces inside the joint. Indeed, only a fraction of cells were seen to remain in the defect in animal studies after the intra-articular injection of stem cells (Muñoz-Criado et al., 2017; Toupet et al., 2013). Therefore the concept of protecting cells with a biomaterial, also serving as a delivery vehicle to the superficial defects, is of growing interest. This biomaterial needs to withstand loads and shear forces, while promoting differentiation of therapeutic cells and production of their own matrix. In principle, hydrogels are potential candidates, as they can be arthroscopically applied, smoothly fill the rough defects, be polymerized at the defect (e.g., by temperature change, UV-crosslinking). In addition, they can even be loaded with therapeutics for an initial boost in differentiation (Koh et al., 2020). However, hydrogels used so far do not sufficiently satisfy these conditions. Alginate, a natural biomaterial frequently used in cartilage research (Häuselmann et al., 1996; Lee et al., 2003), is not suitable for intra-articular application and cannot be degraded by cells to be replaced by new matrix. Fibrin, often used as a tissue glue and for cell encapsulation (Fürsatz et al., 2021; Perka et al., 2000; Salam et al., 2018), can be easily applied but bears low mechanical stability and degrades rapidly.

In contrast, gelatin derived from collagen - a principal constituent of cartilage tissue - exhibits many beneficial properties arising from its chemical structure. Similar to fibrin or collagen, the polymer structure of gelatin includes necessary cell-binding motifs (e.g., Arginine-Glycine-Aspartate [RGD]), allowing for cell adhesion (Van Hoorick et al., 2019). It further provides cleavage-sequences for matrix metalloproteinases rendering the hydrogel biodegradable. Notably, the material is biocompatible, inexpensive, and can be easily modified (Yue et al., 2017). However, as gelatin is soluble at a physiological temperature of 37°C, it needs to be modified and/or cross-linked using functional groups such as methacrylamide, acrylamide, or norbornene to ensure stability at body temperature (Van Hoorick et al., 2019). Of those, methacrylamide-modified gelatin methacryloyl (gelMA) is most interesting, as it is more stable and biocompatible than, for example, acrylamide and less prone to premature crosslinking than, for example, norbornene, in addition to being photo-crosslinkable. This property renders the material tuneable in its rheological properties by controlling the degree of substitution (DS) (i.e., degree of methacrylation), polymer concentration, photoinitiator, and irradiation conditions (Van Den Bulcke et al., 2000; Van Hoorick et al., 2015). GelMA allows for injection and in situ (photo-)polymerization, which is highly beneficial and contributes to ease of use when clinically applied. Our recent work showed that gelMA supports long-term cell culture and differentiation of adipose-derived stromal/stem cell microspheroids produced from immortalized human cells (Žigon-Branc et al., 2019).

While gelMA has been evaluated for the use in cartilage regeneration, many studies rely on the use of cell lines (Zhou et al., 2018), animal derived cells (L. Han et al., 2017; M.-E. Han et al., 2017; Mouser, 2018; Wang et al., 2021) or very young donors (Boere et al., 2014) thus making them less applicable for translational research. Other studies using human chondrocyte sources (Brown et al., 2017; Gu et al., 2020) often focus on material characterization and only superficially describe effects on the cellular level. Also comparisons of differentiation capacity gelMA embedded cells to culture systems routinely used to assess the differentiation potential of cells (e.g., pellet culture), which is especially important for older human donors and later passages is seldomly shown. Furthermore little is known about the use of cell-laden gelMA for the treatment of superficial cartilage damage, for example, found in osteoarthrosis (OA).

Therefore this study examines the suitability of gelMA for chondrocyte differentiation, cartilage regeneration and temporal reconstitution of the gliding surface of superficially damaged cartilage. Specifically, we investigated the viability and extracellular matrix generation potential (on mRNA and protein level) of human articular chondrocytes (hAC) within gelMA and in comparison to

standard pellet culture. The performance on the damaged cartilage surface was assessed on human osteoarthritic cartilage as an ex vivo model under simulated human gait.

2 | METHODS

2.1 | Chondrocyte isolation procedure and cell culture

With written informed consent and approval of the local (Medical University of Vienna; approval number 2127/2017) ethical board hAC were isolated from femoral heads of three donors (male, age: 51–66) undergoing joint-replacement surgery due to trauma. Pieces of macroscopically intact cartilage were cut from the bone and washed in phosphate-buffered saline 1X (PBS, Sigma) containing 10 µg/mL amphotericin B (Gibco) and 0.5 mg/mL gentamicin (Gibco) for 30 min. Subsequently, the pieces were digested for another 30 min in 1 mg/mL hyaluronidase solution (Sigma) and for 1 h in 1 mg/mL pronase solution (Gibco). Then, the cartilage was digested for 3 days in a mixture of enzymes containing 200 U/mL collagenase II (Gibco) and 1 U/mL papain (Sigma) in Dulbecco's Modified Eagle Medium - High Glucose (DMEM-HG; Gibco). The isolated cells were expanded as passage 0 in chondrogenic proliferation medium (CM) under standard cell culture conditions (37°C, 5% CO_2, humidified atmosphere). This medium contained Dulbecco's Modified Eagle Medium - High Glucose (DMEM-HG) (Gibco) supplemented with 10% newborn calf serum (NBCS; Gibco), 2 mM L-glutamine (Sigma), 2 µg/ mL amphotericin B, 100 µg/mL gentamicin, 50 µg/mL L-ascorbic acid 2-phosphate (Sigma), 10 mM HEPES (Corning) and 5 µg/mL insulin (Sigma). Medium was exchanged twice a week. Cells were passaged using Trypsin-EDTA (0.05%, Gibco) at a confluence of 90% and used for encapsulation in passages 3 and 5 (P3 and P5).

2.2 | gelMA preparation

Gelatin methacryloyl was produced as described previously (Ovsianikov et al., 2011; Van Den Bulcke et al., 2000; Van Hoorick et al., 2018). Briefly, gelMA was synthesized using gelatin-type-B from bovine skin as a starting material. To obtain photosensitive material, the amine side groups were chemically substituted with methacrylamide groups through reaction with 1 equivalent methacrylic anhydride yielding a DS of 60%. Purification occurred via dialysis exploiting a cut-off of 12,000–14,000 Da, followed by isolation through lyophilization.

For encapsulation experiments, the photoinitiator lithium phenyl-2,4,6-trimethyl-benzoylphosphinate (Li-TPO) was used. It was synthesized as described in literature (Majima et al., 1991; Markovic et al., 2015).

The precursor solution was prepared by dissolving gelMA in CM at 37°C with occasional vortexing. The photoinitiator, dissolved in PBS, was added to yield a final concentration of 0.3, 0.6, or 1.2 mM.

Experiments containing the light-sensitive photoinitiator were performed protected from light.

2.3 | Phototoxicity of Li-TPO

In order to evaluate the optimal biocompatible concentration photo-toxicity testing of the photoinitiator Li-TPO was performed on hAC. Li-TPO concentration was selected as the highest possible concentration that is not harmful to the cells, yet allows for the highest stiffness and fastest crosslinking of gelMA. Human articular chondrocytes in P3 were seeded in two 96-well plates at a cell density of 7000 cells per well and incubated at 37°C overnight. The next day, medium was removed and the cells were exposed to 100 µL/well of 1.2 mM, 0.6 and 0.3 mM Li-TPO dissolved in CM ($n = 8$). Cells in control wells received either CM without Li-TPO (positive control) or CM with 50% Dimethylsulfoxide (DMSO, negative control; Sigma). One plate was exposed to ultraviolet (UV) light in a UV-chamber (UV-A, 365 nm, 25 mW/cm^2 in a Lite-Box G136, NK-OPTIK, at room temperature) for 10 min to activate the photoinitiator while at the same time the second plate was incubated in the dark at room temperature. Hence, one plate represents the photo-toxicity effect that the irradiated photoinitiator has on the cells and the second plate shows the effects that the inactive photointiator might have on the cells by itself.

Thereafter, both plates were incubated for 2 h at standard cell culture conditions and then the solutions of all wells were exchanged with fresh CM. After 24 h of cell resting period, Presto Blue Metabolic Viability Reagent (Life Technologies) was used to determine the metabolic activity and therefore the degree of phototoxicity. The reagent was diluted 1:10 in CM and 100 µL were added per well. After 1 h of incubation the fluorescence was measured using a plate reader (Synergy H1 BioTek, excitation 560 nm, emission 590 nm). Background fluorescence was corrected according to sample blank, which contained Presto Blue reagent in CM. Cell metabolism of control cells (no Li-TPO; no UV) was defined as 100% cell viability and other conditions where normalized to this control to calculate individual viability for each condition.

2.4 | Photorheology

To characterize the photo-crosslinking characteristics and viscoelastic properties of gelMA, oscillatory shear measurements were performed with aqueous solutions of gelMA with 5%, 7.5%, 10% as well as 12.5% (w/w) of gelMA (in the presence of 0.6 mM Li-TPO as photo-initiator) by means of a photorheometer (MCR 302 WESP, Anton Paar) with a light source of 320–500 nm wavelength and an intensity of 6 mW cm^{-2} (Omnicure) (Gorsche et al., 2017). The samples were assayed using a parallel plate geometry setup, where 60 µL of gelMA precursor solution was loaded between the plates with a gap of 50 µm. Paraffin oil was applied at the edges to prevent drying of the gelMA film during measurements. A frequency of 10 Hz and a strain of 10% was applied via the parallel plates ($d = 25$ mm) at

37°C. The parameters were determined to be within the viscoelastic range of gelMA. The temperature was set at 37°C. Each sample was equilibrated for 20 s before the light source was turned on. Storage- (G′) and loss moduli (G″) were recorded in second intervals.

2.5 | Photo-encapsulation of human articular chondrocytes

Human articular chondrocytes from three human donors were encapsulated at P3 and P5 in 7.5% and 10% (w/w) gelMA in the presence of 0.6 mM Li-TPO via UV-crosslinking. The cells were harvested, counted and suspended in different pre-warmed gelMA (i.e., 37°C) precursor solutions. A cell density of 0.2×10^6 cells per 30 μL gelMA scaffold was used. The scaffolds were formed using chambered coverglass (Grace Bio-Labs CultureWell™) with 6 mm diameter and 1 mm depth. These silicon masks were put on a glass slide positioned on a heating plate (at 37°C) and the cell-loaded gelMA solution was dispensed to each well. Then the silicon mask was covered with a second glass slide. To achieve a physical crosslinking, the gelMA samples were cooled down on ice for 30 s. Then the gelMA scaffolds were chemically crosslinked using UV-A light at 365 nm with an intensity of 25 mW/cm^2 for 10 min. The cross-linked samples were transferred to 48-well plates and washed in CM for 30 min. Then, chondrogenic differentiation medium (CDM), containing different amounts of transforming growth factor-β3 (TGF-ß3; Lonza) was added (0, 1, or 10 ng/mL). Chondrogenic differentiation medium consisted of DMEM-HG supplemented with 100 U/mL penicillin/ streptomycin (Sigma), 2 mM L-glutamin, 0.05 mM L-ascorbic acid 2-phosphate, 5 μg/mL human serum albumin (Sigma), 2.5 μg/mL linoleic acid (Sigma), 5 mg/mL insulin and transferrin and 5 ng/mL selenous acid provided as ITS premix (Gibco), 100 nM dexamethasone (Sigma) and 0 ng, 1 ng, or 10 ng of TGF-ß3. GelMA scaffolds were cultured in 280 μL of CDM, which was exchanged twice a week with freshly prepared medium. The scaffolds were cultured for 3 weeks.

In addition to gelMA embedded samples, standard pellet cultures were included as controls. HAC were suspended in CDM with different amounts of TGF-ß3 (0, 1, or 10 ng/mL) and 0.2×10^6 cells in 280 μL CDM were transferred to 1.5 mL screw-capped polypropylene tubes (Corning). Cells were centrifuged down at 280 x g for 5 min. The screw-caps were subsequently slightly loosened to allow air exchange, and tubes were placed into the incubator. Compact pellets formed overnight and were treated the same way as experimental gelMA samples. After 5 days, the cell pellets were transferred to 96-U-bottom well plates.

2.5.1 | Live dead staining

Prior to performing live-dead staining, gelMA scaffolds were washed 3 times in PBS. The staining solution was applied, containing 0.6 μM propidium iodide (Life Technologies) and 0.4 mM calcein-AM (Life Technologies) in PBS. These were incubated for 30 min at standard cell culture conditions and then washed again in PBS. Stained samples were transferred to 35 mm imaging dishes with glass bottom (ibidi) and imaged in PBS. Three dimensional (3D) images were generated from z-stacks taken at excitation/emission sets of 488/ 530 nm (green fluorescence of live cells) and 530/580 nm (red fluorescence of dead cells) with the laser scanning microscope (LSM700, Zeiss), with scanning a range of 400 μm.

2.5.2 | RNA isolation and quantitative reverse transcriptase polymerase chain reaction

After 21 days of culture, samples of the differentiation experiment were harvested and RNA was isolated. To ensure a sufficient RNA yield, three cell-loaded gelMA scaffolds were pooled. The cell-loaded gelMA scaffolds were shock frozen in liquid nitrogen and afterward grinded within the microcentrifuge tube using a micropestle. 900 μL of Quiazol Lysis Reagent (Quiagen) were added to the tube. RNA was isolated using RNeasy Plus Universal Mini Kit (Quiagen) following manufacturer's instructions. For control pellets, three pellets were pooled. Pellets were incubated overnight in Quiazol Lysis Reagent prior to RNA isolation. For all samples, the yield and purity of RNA were evaluated using a NanoDrop 2000c photometer (Thermo Scientific). RNA samples were purified using AccuRT Genomic DNA Removal Kit (abm) and 700 ng per sample were used to synthesize cDNA using 5X All-In-One RT MasterMix (abm).

Quantitative reverse transcriptase polymerase chain reaction (qRT-PCR) was performed in duplicates using SsoAdvanced Universal SYBR® Green Supermix (BioRAD) and primer mixes also obtained from BioRAD. To analyze the status of redifferentiation, the following genes were investigated: collagen type I, α-1 (COL1A1, qHsaCED0043248), collagen type II, α-1 (COL2A1, qHsaCED0001057), aggrecan (ACAN, qHsaCID0008122), versican (VCAN, qHsaCID0023082). β-2-micro-globulin (B2M, qHsaCID0015347) was used as housekeeping gene. The qRT-PCR analysis was carried out on a CFX 96 Connect Real-Time System (BioRAD) and the cycling program was set as follows: polymerase activation and initial denaturation (30 s at 95°C) followed by repeated denaturation (15 s at 95°C) and annealing/extension (15 s at 60°C) for a total of 40 cycles. The melt-curve analysis followed by increasing the temperature from 65°C to 95°C (0.5°C increment for 5 s/step).

The ΔΔCt method was used for analysis and data was processed using CFX Manager Version 3.1 (BioRad). Ct values of samples were normalized to the housekeeping gene and referenced to time point 0, which represents the day of encapsulation (RNA harvested from 2D monolayer cell culture before encapsulation). For calculations of differentiation indices, ratios of COL2/COL1 and ACAN/VCAN were calculated. Therefore, the geometric means of three biological replicates ($2^{-\Delta\Delta Ct}$) were used.

2.5.3 | Histology

After 21 days in culture, pellets and gelMA scaffolds were washed in PBS and fixed for 24 h in 4% formalin (Roth). Then, samples were

washed in PBS several times for 1 h and dehydrated starting with 50% ethanol following a series of increasing ethanol concentration and final embedding in paraffin using Tissue Tek VIP (Sakura). Samples were cut to obtain sections of 4 μm thickness. Sections were deparaffinized and stained with Alcian blue (0.3% at pH = 2.5) to determine the presence of glycosaminoglycans (GAG) and with collagen type II antibodies (Thermo Fisher Scientific, clone 6B3) for presence of collagen type II. For immuno-staining BLOXALL (Vector Labs) was used as a blocking reagent for endogenous peroxides and alkaline phosphatase, followed by antigen retrieval using pepsin (pH = 2). Subsequently, sections were incubated with a 1:100 dilution of primary antibody for 1 h at room temperature, followed by BrightVision Poly-HRP (VWR) as secondary antibody. For detection NovaRed (Vector Labs) was used. Nuclear counterstaining was performed using Mayer's hematoxylin.

2.6 | Cartilage specimen preparation for sealing tests

Full-depth osteochondral plugs of OA cartilage of 10 mm diameter were harvested from human femoral heads. To obtain a uniform height, the initial plugs were shortened using a table saw, yielding a length of ~8 mm. The OA plugs were coated with 10% gelMA containing: (1) hAC-DiO (hAC were labeled green with Vybrant DiO cell-labeling solution [ThermoFisher Scientific] prior encapsulation, according to manufacturer's instructions) (P1), (2) hTERT immortalized human adipose-derived mesenchymal stem cells (MSC) (ASC/TERT1, Evercyte) transduced with green fluorescent protein (GFP) as explained elsewhere (Knezevic et al., 2017), and (3) a co-culture (1:1) of hAC-DiO (green) and mCherry (red fluorescent protein) transduced ASC/TERT1 (red) (Knezevic et al., 2017). Therefore, freshly isolated primary hAC, were used after 5 days of monolayer-culture. ASC/TERT1-GFP and ASC/TERT1-mCherry were expanded in Endothelial Cell Growth Medium-2 (EGM-2, Lonza). Co-cultures were cultured in Hennig's medium containing DMEM-HG supplemented with 100 U/mL penicillin/streptomycin, 2 mM L-glutamine, 5 mg/mL insulin and transferrin and 5 ng/mL selenous acid provided as ITS premix, 0.17 mM ascorbic acid-2-phosphate, 1 mM sodium pyruvate (Gibco), 0.35 mM L-proline (Sigma), 1.25 mg/mL bovine serum albumine (BSA; Sigma) and 0.1 μM dexamethasone (Nürnberger et al., 2019). A cell density of 0.4×10^6 per 30 μL was used.

For coating, the plugs were placed into custom-built silicon molds. The surface was dried with a sterile paper towel and the liquid cell-loaded gelMA precursor solution was applied. A transparent plastic coverslip was put atop, to overcome capillary forces of the mold walls, and the precursor was crosslinked for 10 min with UV light. The plastic coverslip was peeled off afterward and samples were submerged in the respective medium: hAC in CM, ASC/TERT1 in EGM-2, and co-cultured cells in Hennig's medium supplemented with 1 ng/mL TGF-ß3 and 1 ng/mL human BMP-6 (R&D Systems). After 30 min, medium was exchanged and samples were cultured

overnight. On the next day, cells were stained with ethidium-homodimer-1 (Life Technologies) to visualize dead cells. Plug samples were cut in half, to observe the sealing effect of gelMA and cellular distribution and Z-stack images of cross-sections were taken using confocal microscopy (LSM700, Zeiss).

2.7 | Mechanical stress tests

A mechanical stress test, simulating the mechanics of human gait within the knee joint, was performed using a tribometer (SRV® test rig (tribometer), Optimol Instruments Prüftechnik) (Göçerler et al., 2019). Osteochondral plugs coated with cell-loaded gelMA containing hAC-DiO (0.4×10^6 cells per 30 μL) were used for testing. After coating as described above, the cartilage portion of the 10 mm plugs was cut using an 8 mm biopsy punch, to remove excess tissue/gel and yield sharp edges. Samples were exposed to mechanical stress using the SRV® test rig (see Figure 6e), in which two samples were loaded against each other. Each plug was placed in one sample holder and the liquid cup was filled with DMEM-HG supplemented with 10% NBCS. The upper and lower sample holder were assembled by placing the two specimen on top of each other. To equilibrate the samples, they were pre-loaded within about 1 s with a normal force of 50 N for 30 min at 37°C (external heating of the liquid cup). Following this phase, the normal load was increased to 180 N within about 1 s. The normal load of 180 N corresponds to a nominal contact pressure of ~3.5 MPa, which simulated human gait (Patil et al., 2014; Yoon et al., 2018). Thereafter, the samples were linear oscillating against each other for ±0.5 mm (1 mm peak to peak, respectively 2 mm per cycle, in total 600 mm sliding path) at a constant relative velocity of 1 mm/sec for 10 min. Then the load was decreased within about 2 s to about 1 N (unloading) for 10 min to stimulate reabsorption of fluid into the system, without losing the contact completely. Loading and unloading were repeated for two more repetitions. All measurements were performed at 37°C (external heating of liquid cup) and the tangential force (resistance to the linear oscillating movement) in the contact zone was monitored continuously over time to calculate the coefficient of friction (per definition: tangential force divided by normal load).

To evaluate, if the encapsulated hAC-DiO survived the mechanical stress, samples were stained with ethidium homodimer-1 immediately after the measurement. Samples were afterward fixed with 4% paraformaldehyde overnight, washed with PBS and analyzed via confocal-microscopy as described above.

2.8 | Statistical analysis

Data were analyzed with IBM SPSS Statistics 24. The normal distribution of data was confirmed using the Shapiro-Wilk test and Q-Q-Plots. The Levene test verified the equality of variances in the samples.

To analyze whether the photoinitiator (with or without activation by UV light) had adverse effects on the metabolic activity of hAC, one-way analysis of variance (ANOVA) was performed. For post-hoc comparison a two-sided many-to-one Dunnet-test was used to compare all groups against the control group without UV irradiation (-UV).

Gene expression of *COL2* for passage 3 was analyzed using a mixed model ANOVA: The different culture conditions (10%, 7.5% gelMA and pellet culture) and the different growth factor concentrations (0, 1 or 10 ng/mL TGF-ß3) were considered repeated measures variables and the donor was considered the between group variable. $p < 0.05$ was considered statistically significant.

3 | RESULTS

We investigated the feasibility of a photo-crosslinkable hydrogel gelMA for use in cartilage tissue engineering. Specifically, we evaluated its cytocompatibility, mechanical properties, and feasibility as environment for chondrocyte redifferentiation. Furthermore, we investigated its applicability on cartilage surfaces and performance under mechanical stress in vitro.

3.1 | Phototoxicity of Li-TPO

In order to assess the optimal concentration of the photoinitiator for gel crosslinking and cell encapsulation, phototoxicity testing was performed by exposing hAC in 2D culture to different concentrations of Li-TPO (0.3, 0.6, and 1.2 mM) with and without UV irradiation (Figure 1), and assessing cell metabolism, indirectly reflecting cell survival and toxicity. Concentrations of 0.3 and 0.6 mM Li-TPO did not adversely affect cell metabolic activity compared to untreated control samples, independent of UV light exposure. However, the highest tested concentration (1.2 mM) reduced metabolic activity to 88% (without UV) and 72% for hAC exposed to UV ($p < 0.001$). Overall, 0.6 mM Li-TPO was the highest photoinitiator concentration, without adverse effects on cell metabolism activity, while also enabling efficient crosslinking and was therefore used in all further experiments.

3.2 | Photorheology

The crosslinking dynamics and viscoelastic properties of gelMA were analyzed via oscillatory shear rheology measurements during curing of the hydrogel. Storage- (G′) and loss-moduli (G″) were measured as the material responds to the irradiation over a curing time of 10 min (Figure 2). Immediately upon UV irradiation, gelMA began to crosslink. The gel point, where G′/G″ equals 1, defining the transformation of a materials liquid to solid state, was reached within 20 s, except for 5 wt% gelMA, which needed 40 s. After 3 min about 70% and after 5 min about 80% of the final G′ (measured after 10 min) was attained except for 5%. Formulations containing 5% gelMA developed inferior mechanical
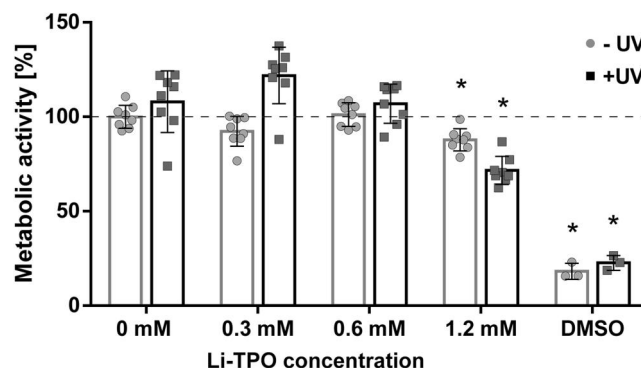

FIGURE 1 Metabolic activity of human articular chondrocytes (P3) exposed to different concentrations of lithium phenyl-2,4,6-trimethyl-benzoylphosphinate (Li-TPO) with and without exposure to UV light. Metabolic activity was measured by resazurin-based Presto Blue staining after 2 h of Li-TPO exposure followed by 24 h of incubation. Presto Blue fluorescence of cells treated with different Li-TPO concentrations is shown as mean percentage ± standard deviation compared to control (no Li-TPO). $n = 8$ for each group. * highlights significant differences ($p < 0.001$) compared to control -UV. There was no difference between the 0.6 mM Li-TPO and control groups. (Dimethylsulfoxide [DMSO] = negative control, $n = 3$)

properties with only 0.204 kPa ($\pm 9.2 \times 10^{-3}$ kPa) storage modulus at the end of the measurements after 10 min, compared to the other gelMA concentrations (7.5%, 10%, 12.5%). G′ for the other gelMA concentrations showed values of 1.7 kPa (± 0.000 kPa) for 7.5% gelMA, 4.5 kPa (± 0.240 kPa) for 10% gelMA and 10.5 kPa ($\pm 0.212 \times 10^{-3}$ kPa) for 12.5% gelMA. As we found that the mechanical stability of 5% gelMA was inferior and that the viscosity of 12.5% gelMA was too high for efficient handling with cells, 7.5% and 10% gelMA were chosen for further encapsulation studies.

3.3 | Encapsulation of human articular chondrocytes

Primary hAC from three different donors were propagated in 2D-culture until P2 or P4 prior to encapsulation in 7.5% (further in the text referred to as soft) or 10% (further in the text referred to as stiff) gelMA, and cultivated (P3 and P5) for another three weeks in medium containing 0, 1 or 10 ng/mL TGF-ß3. Chondrocytes were then analyzed for viability, morphology, gene expression profile, and synthesized matrix (glyco-)proteins. Samples were compared to controls, that is, pellet cultures, which also contained hAC from the three donors.

3.3.1 | Live/dead staining

To assess viability and morphology of hAC within gelMA after three weeks of encapsulation, cells were analyzed using live-dead staining.
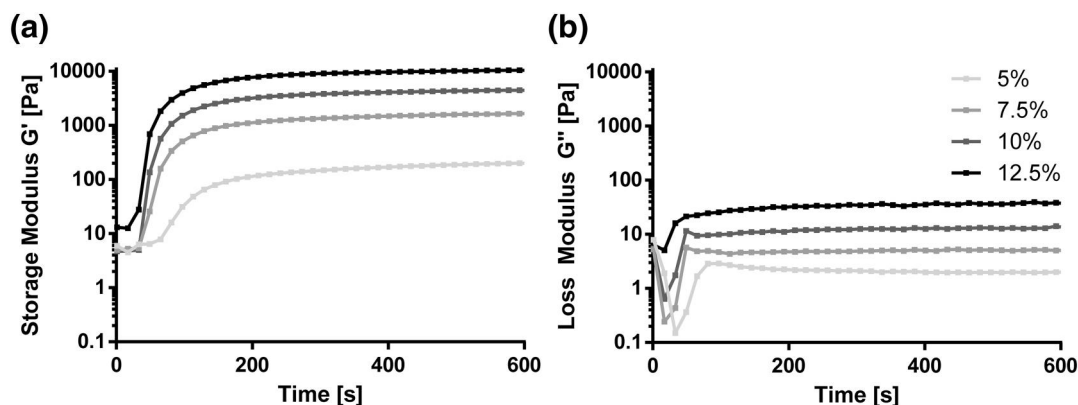
FIGURE 2 Rheological measurements of 5%, 7.5%, 10%, and 12.5% wt% gelatin methacryloyl (gelMA) with 0.6 mM lithium phenyl-2,4,6-trimethyl-benzoylphosphinate. Storage-(G′) and loss-moduli (G″) were monitored during oscillatory time sweep over 10 min ($n = 2$) of UV-irradiation using a photorheometer at 37°C. UV irradiation started after 20 s of measurement. G′ and G″ are shown as the mean of two measurements. Storage modulus of 12.5% gelMA resulted in highest stiffness (10.5 kPa) followed by 10% (4.5 kPa), 7.5% (1.7 kPa), and 5% (0.204 kPa)

HAC were highly viable in all investigated gelMA formulations and only few dead cells were detected.

HAC cultured in medium containing 10 ng/mL TGF-ß3 were homogeneously distributed and had similar morphology regardless of the gelMA stiffnesses. Cells had either the typical round shape found in native cartilage or were polygonal with small cell processes. However, the stiffness of gelMA did affect the cultivation of hAC in the absence of TGF-ß3 (Figure 3) and 1 ng/mL TGF-ß3 (data not shown). In both growth factor conditions, the spindle-shaped, elongated cell morphology typical for the fibroblast phenotype predominated in the soft (7.5%) gelMA, whereas in the stiff condition a round cell shape was more prevalent.

3.3.2 | qRT-PCR

Gene expression of chondrogenic differentiation markers (*COL1, COL2, ACAN, VCAN*) obtained from P3 and P5 hAC encapsulated within gelMA revealed a redifferentiation pattern similar to pellet cultures, which served as a control. For analysis of the overall effect of hydrogel stiffness/culture system and TGF-β3 concentrations, a mixed model ANOVA was performed using two different donors (1 and 3, the two most different donors chosen due to model complexity) as a random factor.

In general, when comparing gelMA scaffolds to pellet cultures a comparable state of differentiation could be achieved. When analyzing *COL2* gene expression on the overall level, a significant TGF-β3 dose dependent upregulation ($p = 0.003$), which was similar in all pellet culture and both gelMA stiffnesses (especially when using 10 ng/mL TGF-β3), could be observed. This behavior was present in both donors and was consistent until P5, however the total amount of upregulation varied between donors. At lower growth factor concentrations differences between systems (gelMA vs. pellet culture) became more apparent. Medium without TGF-ß3 (0 ng/mL) yielded low *COL2* expression. While in most pellet culture samples a
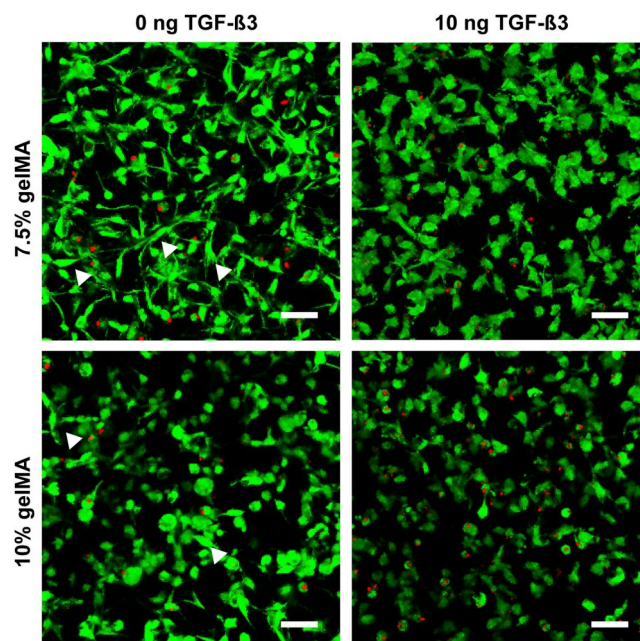

FIGURE 3 Cell morphology of human articular chondrocytes P3 after 3 weeks of encapsulation in soft (7.5%) and stiff (10%) gelatin methacryloyl (gelMA) with and without TGF-ß3. Without TGF-ß3, cell morphology was highly heterogenous in both soft as well as stiff gelMA. Although spindle-shaped (arrow heads) and round cells were found in both stiffnesses, the round cell morphology (chondrocyte like) was favored in the stiffer gelMA, whereas the spindle-like morphology (fibroblast like) was dominant in the softer gelMA. In the 10 ng TGF-ß3 group both stiffnesses contained a rather homogenous cell population of roundish or polygonal cells with little cell processes. Scale bar: 50 μm [Colour figure can be viewed at wileyonlinelibrary.com]

slightly increased differentiation could be observed (in comparison to gelMA), in some cases equal or lower expression (Donor 1 P3, 7.5% gelMA; Donor 1 P5, 10% gelMA; Donor 3 P5, 10% gelMA vs. pellet culture) was found. The most significant differences between gelMA

and pellet culture were observed when using 1 ng/mL TGF-β3. Except for Donor 1 (where the expression was similar) pellet culture was showing stronger *COL2* expression than both gelMA concentrations. The differences described here were not significant when only looking at hydrogel stiffness/culture ($p = 0.058$), but showed significant differences when allowing for factor interaction between gel stiffness/culture system (gelMA, pellet culture), growth factor and donor ($p = 0.007$) in a mixed model ANOVA.

As Donor 3 (P3) responded the strongest to differentiation stimuli this donor's data is presented as an example of gene expression changes after re-differentiation, compared to the hAC de-differentiated state at the time-point of encapsulation (Table 1 and Figure 4; data from other donors is available in Section 1.2 in Supporting Information S1). Changes in gene expression were similar between gelMA and pellet culture, especially when 10 ng/mL TGF-β3 was added, resulting in a strong upregulation of *COL2* (7.5%: 1.9×10^5, 10%: 2.1×10^5 and pellet culture: 0.9×10^5) and to a lesser extent also *COL1* (7.5%: 20.5, 10%: 39.0 and pellet culture: 34.5), ACAN (7.5%: 64.1, 10%: 128.8 and pellet culture: 53.2) and *VCAN* (7.5%: 3.1, 10%: 4.2 and pellet culture: 3.0). Interestingly, at 1 ng/mL TGF-β3 pellet culture (P3) not only showed stronger gene expression in all analyzed genes compared to gelMA, but also stronger expression of *COL2* and *ACAN* than using 10 ng/mL TGF-β3 (pellet culture). Cultures without additional growth factors showed only minimal upregulation of *COL2* in gelMA (7.5%: 2.4 fold and 10%: 1.3 fold) and slightly higher upregulation in pellet culture of P3 (131.5). *COL1*, *ACAN* and *VCAN* were slightly downregulated in most cases. When no growth factor was added, differentiation indices followed this trend with low but positive differentiation (*COL2/COL1*: 7.5%: 3.5, 10%: 2.4 and pellet culture: 426.1; *ACAN/VCAN*: 7.5%: 0.6, 10%: 0.8 and pellet culture: 2.6), and increasing differentiation with 1 ng/mL (*COL2/COL1*: 7.5%: 225.9, 10%: 212.1 and pellet culture: 6.3×10^3; *ACAN/VCAN*: 7.5%: 3.9, 10%: 6.8 and pellet culture: 34.0)

and 10 ng/mL (*COL2/COL1*: 7.5%: 11.4×10^3, 10%: 5.5×10^3 and pellet culture: 2.3×10^3; *ACAN/VCAN*: 7.5%: 19.3, 10%: 31.3 and pellet culture: 17.1) TGF-β3 concentrations, with the exception of 1 ng/mL TGF-β3 in pellet culture showing the strongest differentiation of all conditions.

Weakly responding donors (presented in Section 1.2 in Supporting Information S1) generally followed the same differentiation trend of TGF-β3 dose-dependent increase (mentioned above), but showed significantly lower expression levels for all analyzed genes. This observation was especially true for *ACAN* and *VCAN* where (in low growth factor) media a reduced expression (compared to day 0 levels) was visible.

3.3.3 | Histology

Gelatin methacryloyl encapsulated hAC and pellet culture were histologically analyzed after 21 days in culture and sections were stained with Alcian blue to verify the presence of GAG and antibodies against collagen type II.

Histological stainings reflected the results obtained in qRT-PCR showing mostly no differences between hydrogel stiffnesses. In one donor (Donor 2), however, the stiff hydrogel stained slightly stronger (Sections 1.3.5 and 1.3.6 in Supporting Information S1). Nevertheless, changes in TGF-β3 concentration showed far stronger effects. Cultures exposed to 0 ng/mL TGF-β3 were negative for both GAG and collagen type II irrespective of culture type. Using 1 ng/mL, TGF-β3 both pellet culture and gelMA cultures showed increased GAG deposition, but no collagen type II deposition in most cases. Only hAC from Donor 3 exhibited some collagen type II in pellet culture (Sections 1.3.1 and 1.3.2 in Supporting Information S1) and in individual cells embedded in gelMA. However, in P5 this effect was weaker in pellet culture and wholly absent in gelMA. When 10 ng/mL TGF-β3

TABLE 1 Relative changes in gene expression (fold) after 3 weeks of hAC encapsulated in gelMA or pellet culture compared to day 0 (= time point of encapsulation) for the chosen Donor 3 P3

gelMA concentration /culture model	TGF-β3 concentration	COL2	COL1	Differentiation index (COL2/COl1)	ACAN	VCAN	Differentiation index (ACAN/VCAN)
7.5%	0 ng/mL	2.4	0.8	3.5	0.7	0.7	0.6
	1 ng/mL	1.9×10^3	10.9	225.9	2.9	0.7	3.9
	10 ng/mL	1.9×10^5	20.5	11.4×10^3	64.1	3.1	19.3
10%	0 ng/mL	1.3	0.5	2.4	0.4	0.6	0.8
	1 ng/mL	2.8×10^3	14.1	212.1	8.1	1.2	6.8
	10 ng/mL	2.1×10^5	39.0	5.5×10^3	128.8	4.2	31.3
Pellet culture	0 ng/mL	131.5	0,3	426.1	1.3	0.5	2.6
	1 ng/mL	1.9×10^5	32.8	6.3×10^3	63.2	2.0	34.0
	10 ng/mL	0.9×10^5	34.5	2.3×10^3	53.2	3.0	17.1

Abbreviations: *ACAN*, aggrecan; *COL1*, collagen type I; *COL2*, collagen type II; gelMA, Gelatin methacryloyl; hAC, human articular chondrocytes; *VCAN*, versican.
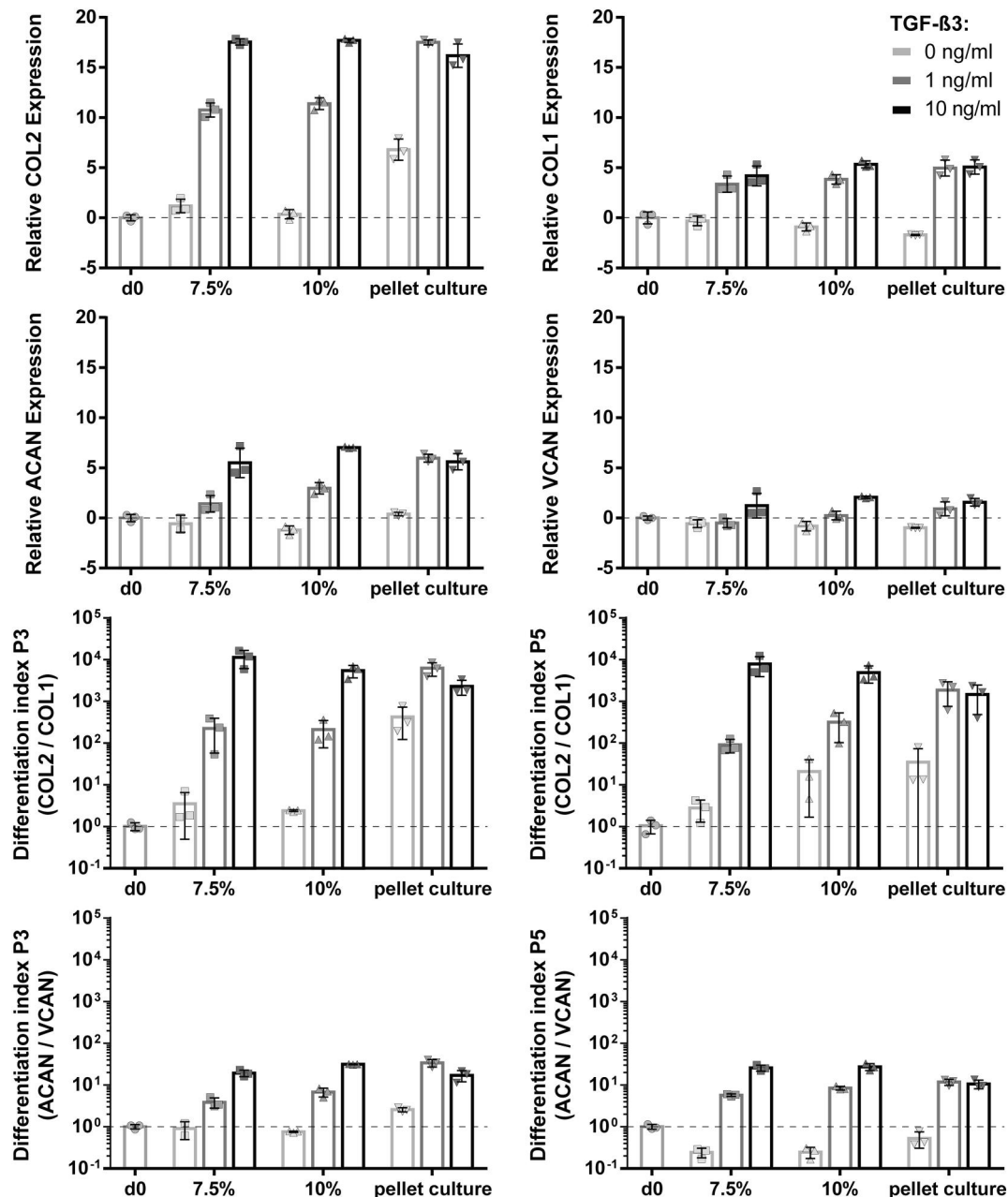
FIGURE 4 Gene expression of chondrogenic markers expressed by human articular chondrocytes (hAC) (Donor 3) encapsulated in gelatin methacryloyl (gelMA) and cultivated under different conditions for 21 days. Cells encapsulated in P3 or P5 in either soft (7.5%) or stiff (10%) gelMA and cultivated in 0, 1 or 10 ng/mL TGF-ß3. As a control, hAC were cultured in pellet culture. Differentiation indices calculated from *COL2/COL1* and aggrecan (*ACAN*)/versican (*VCAN*) are shown. Culture in 10 ng/mL TGF-ß3 showed upregulation of all genes. Cells cultured within gelMA with 10 ng/mL TGF-ß3 showed similar differentiation indices when compared to control (pellet culture). Culture within lower concentrations yielded in lower gene expression of gelMA in comparison to pellet culture. In P5 a similar potential to re-differentiate chondrocytes was found as in P3

was used to stimulate differentiation, all donors exhibited enhanced GAG and collagen type II expression, though the intensity was highly donor dependant. Interestingly, while in qRT-PCR the pellet culture of Donor 3 showed similar expression of *COL2* as other donors, and was the only donor to show collagen type II expression at 1 ng/mL in histological sections, in pellet culture it showed reduced collagen type II protein expression. In contrast, histological analysis of gelMA

cultures showed the highest collagen type II and GAG expression in Donor 3 hAC. This is consistent with qRT-PCR data where Donor 3 showed much higher *COL2* expression in gelMA cultures than other donors.

While both, gelMA and pellet cultures (in all three donors), showed similar response patterns to different TGF-β3 concentrations (regarding staining intensity) the structure and distribution of cells
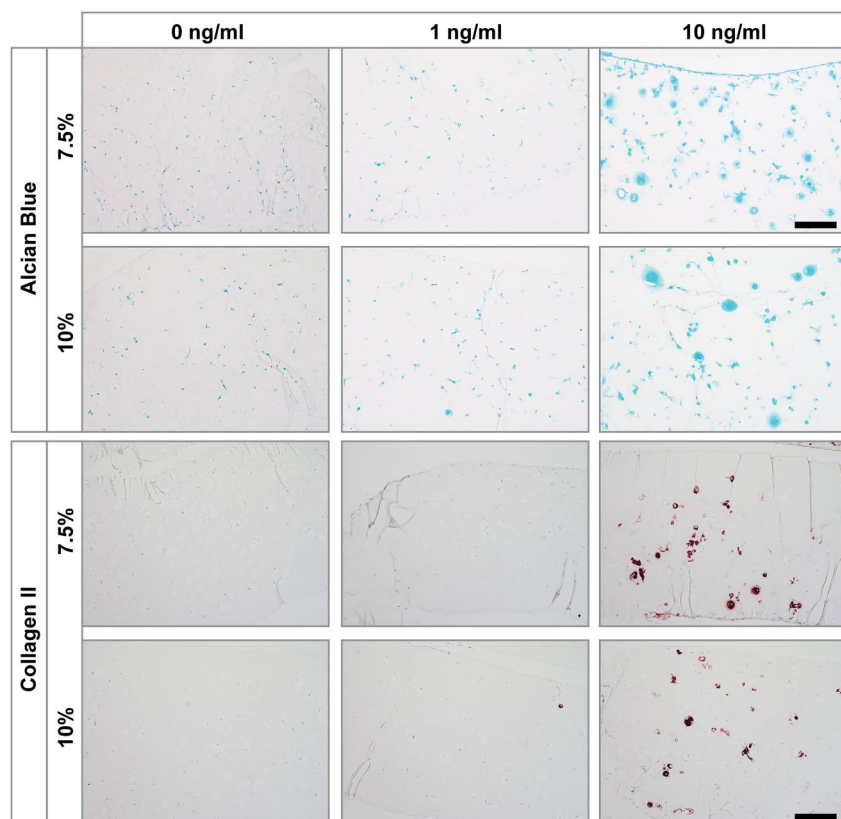
FIGURE 5 Alcian blue and collagen type II stainings of human articular chondrocytes (hAC) (P3, Donor 3) encapsulated in soft (7.5%) and stiff (10%) gelatin methacryloyl (gelMA) after 21 days in culture containing different concentrations of TGF-ß3 (0, 1 and 10 ng/mL). Culture with 0 ng/mL and 1 ng/mL TGF-ß3 displayed a lack of collagen type II staining. Glycosaminoglycans staining was absent in 0 ng/mL TGF-β3 cultures but showed slight staining at 1 ng/mL TGF-β3. HAC cultures within 10 ng/mL TGF-β3 both stainings clearly showed positive cells. The staining was located in close proximity to the cells and within the gelMA matrix. Scale bar: 100 µm [Colour figure can be viewed at wileyonlinelibrary.com]

and matrix differed strongly. In pellet culture the differentiation could be observed in smaller patches and cells were packed together rather densely, only slightly separated by the secreted extracellular matrix. In contrast, in gelMA single cells or small clusters (2–4 cells) were separated by the hydrogel, resembling the structure found in native cartilage, and exhibited staining surrounding the cells. In case of strongly differentiating cells (Donor 3, Figure 5; 10 ng/mL TGF-β3) GAG and collagen type II were not only found in the immediate cell surroundings, but were deposited into the initial hydrogel.

3.4 | Sealing of OA osteochondral plugs

In order to test the performance of gelMA as a sealant for OA cartilage, osteochondral plugs of OA cartilage with superficial damage and tissue loss were used as a model. The surface of plugs was coated with a cell-loaded gelMA (10%) to fill ridges and furrows, replacing the lost tissue and recover its smooth surface. GelMA was loaded with hAC (DiO-labeled) and ASC/TERT1-GFP, which were used as a more easily available model for primary ASC (which present a suitable alternative cell source for cartilage regeneration (Bielli et al., 2016; Erickson et al., 2002)). It was possible to create a layer of gelMA, infiltrating the superficial irregularities of the cartilage matrix, thereby replacing the degraded tissue (Figure 6). GelMA adhered well to the cartilage matrix and formed a stable layer containing cells with spherical morphology. To analyze cell viability, mono-cultures of hAC and ASC/TERT1 were stained with ethidium homodimer-1, visualizing the nucleus of dead cells in red (Figure 6a,b). In both cell types, few dead cells could be observed, demonstrating that encapsulation and application procedures are cytocompatible. DiO labeled hAC and ASC/TERT1 were applied to the osteochondral plugs (Figure 6c,d) to validate the possibility of embedded cultures. Cross-sectional imaging showed a homogeneous distribution of both cell-types within the coating layer.

3.5 | Mechanical stress tests

To test the behavior of cell-loaded gelMA under mechanical stress, we used a tribometer to simulate the sliding movement in a tribological loaded contact during human gait by rubbing OA-osteochondral plugs coated with cell-laden gelMA against each other (Figure 6e) (Göçerler et al., 2019). We found that, after mechanical simulation of human gait with 3.5 MPa and 1 mm/sec, the gelMA layers of both samples (upper and lower part) stayed intact (Figure 6f,g). To see if gelMA protected the cells from the applied mechanical stress, samples were stained for viability (Figure 6h).

The normal load and tangential force (to calculate the coefficient of friction) was monitored every second over the course of the measurement. After initial decrease from 0.016 to 0.006 during the first load-and-movement cycle, the coefficient of friction settled at a value of 0.006 with a standard deviation of $\pm 6.5 \times 10^{-4}$ (mean value of all monitored values in the second and third repetition of loading). Due to the contact geometry and the elasticity of the samples, it has to be pointed out that the measured tangential force is a combination of friction force and a force to overcome the elastic material deformation, especially during the running-in after the first loading.
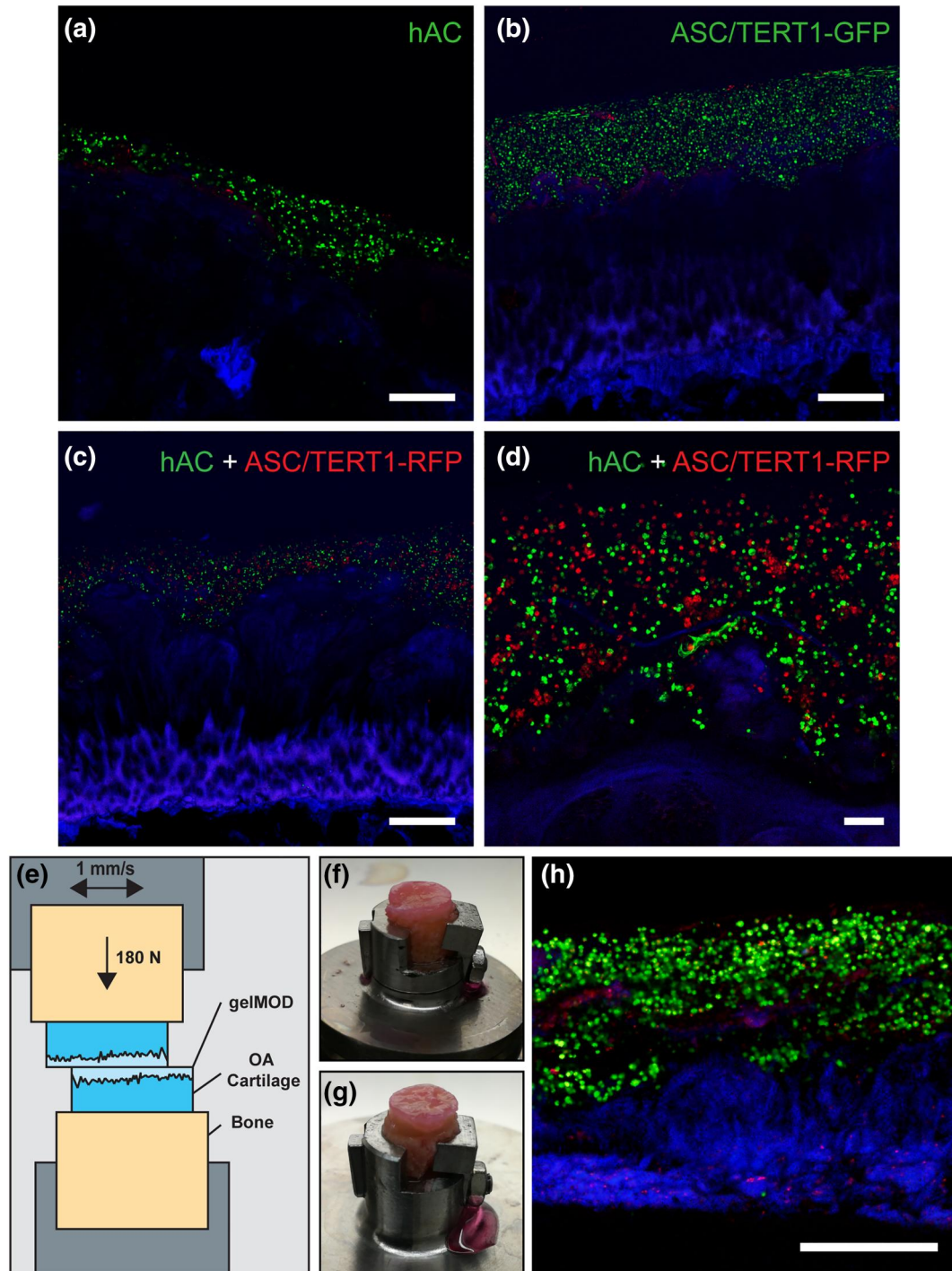
FIGURE 6 Superficially damaged osteoarthritis (OA) cartilage coated with cell-loaded gelatin methacryloyl (gelMA) (10%) after 1 day of cultivation and after simulation of human gait. (a) gelMA loaded with human articular chondrocytes (hAC) (DiO, green) and stained for dead cells (ethidium homodimer 1; red) on cartilage (autofluorescence; blue). (b) gelMA loaded with ASC/TERT1-GFP (GFP-transduced; green) and stained for dead cells (ethidium homodimer 1; red) (c) Overview and (d) detail of co-culture of hAC (green) and ASC/TERT1-mCherry (red). Scale bar: (a–c) 500 μm and (d) 100 μm. (e) Schematic of the experimental setup for the mechanical simulation of human gait. Osteoarthritic specimens were coated with cell loaded (hAC-DiO) gelMA (10%) and exposed to mechanical stress to simulate human gait. The gelMA layer stayed intact in both specimens: (f) lower specimen of the measurement, (g) upper specimen. (h) Live/Dead staining of a cross-section of the lower specimen showing living cells (green), dead cells (red) and cartilage (blue). Scale bar: 500 μm [Colour figure can be viewed at wileyonlinelibrary.com]

4 | DISCUSSION

Cartilage is a tissue with a low intrinsic regeneration potential. So far the most frequently used treatment modalities are unsuitable for superficial cartilage defects, as present, for example, in OA. The main problem is the fixation of the cells and/or scaffolds in shallow defects. This is especially hard for sponge-like or fibrous materials (Alves da Silva et al., 2010), as the material ideally needs to adhere to the defect and fill small crevasses. Other materials, using physical crosslinking (e. g., acid-soluble collagen) produce hydrogels, which are able to fill such defects (Chen et al., 2013), but need high protein concentrations to reach comparable stiffnesses, and need cooling to prevent premature gelation. Therefore, innovative solutions are needed to overcome these problems. There are many different materials currently in development for the treatment of cartilage defects, with only a fraction fulfilling the necessary characteristics for the treatment of superficial cartilage defects (Wei et al., 2021). Here we investigate the potential use of a photo-polymerizable gelMA hydrogel as a bio-compatible, biodegradable and injectable hydrogel for cartilage regeneration appearing especially promising for this application. Due to its characteristics such as a short gelation time (2–10 min) and adhesiveness to damaged tissue (Assmann et al., 2017), it allows for easy and accurate administration of therapeutic cells. Due to the covalent bonds created by photo-crosslinking, gelMA exhibits superior stability and mechanical properties compared to physically crosslinked (e.g., by ions or hydrophobicity) hydrogels (Liu et al., 2017). Furthermore, while being biodegradable, its stability is higher than many other covalently crosslinked hydrogels frequently used in clinics (e.g., fibrin), which often degrade within a few weeks (Wolbank et al., 2015). Even though functionalized fibrins have improved material characteristics for cartilage repair (Almeida et al., 2016), degradation behavior is still not ideal without additional crosslinking. The stability of gelMA allows for more extended protection of delivered cells from harmful external influences. Additionally, it is an important factor for cartilage regeneration, as hydrogels should initially support tissue formation and differentiation and later degrade at an appropriate rate so that the cells can simultaneously produce their own matrix and re-establish normal function. This balance is not possible for hydrogels such as alginate, which is not degradable in its unmodified form and therefore unsuitable for this kind of use. Modification of these materials (Park & Lee, 2014) and use of biodegradable synthetic materials reduce some of these issues, however concerns about degradation products remain when thinking about clinical application.

Within this study we investigated the differentiation capacity of hAC (P3 and P5), which was slightly reduced in P5 when embedded in both formulations of gelMA (soft: 7.5% and stiff: 10%) as well as in the biomaterial-free culture form of pellet culture (i.e., a standard way of culturing for redifferentiation assays). Generally, differentiation of hAC in gelMA and pellet culture was determined by the growth factor concentration and little influenced by the culture system. Without addition of growth factors almost no redifferentiation could be achieved, with slightly better performance of pellet culture and stiff gelMA in comparison to soft gelMA hydrogels

in some of the donor cells and passages. Even though sufficiently stiff gels have previously shown to also induce differentiation without the addition of growth factors (Allen et al., 2012), these results were achieved with non-human cells, which have a higher redifferentiation potential due to species or age. Nevertheless, even under these conditions significantly higher differentiation was achieved in synergy with TGF-β (Allen et al., 2012). As we used cells from older human donors (51–66 years old) the effect of gel stiffness was likely not sufficient to induce re-differentiation by itself. However, what we did observe is that without additional growth factors stiff gelMA was able to induce a rounded cell morphology, which is closer to the physiological morphology of differentiated chondrocytes, which has previously been shown for other types hydrogels (Li et al., 2016).

When adding growth factors to the medium, the differentiation of hAC in gelMA and pellet culture was significantly enhanced. A concentration of 10 ng/mL TGF-β3 was used as a stimulus to analyze the maximal differentiation potential of donor cells. With this high dose, gelMA embedded cells showed similar or even upregulated gene expression of chondrogenic markers (COL2, ACAN) than pellet culture, while histological stainings revealed the deposition of matrix into the hydrogel (Donor 3). Due to the material density it was mainly located in the circumference of chondrocytes, which leads to a chondron-like appearance. The pericellular deposition exhibited in gelMA was similar to what has been previously described for dense fibrin and alginate (Almqvist, 2001; Bachmann et al., 2020). Due to the lower degradation rate of gelMA compared to fibrin, in the long run, cells would have more time to replace the scaffold while it is degraded which might be favorable for defect regeneration. However, higher cell numbers might be necessary if deposition zones cannot grow large enough to fully overlap. As TGF-β3 is a potent stimulus for chondrogenic differentiation, it might mask possible positive differentiation effects of the embedding hydrogel. Therefore, a concentration of 1 ng/mL TGF-β3 was tested in order to give cells growth factor stimulus without masking other effects, a problem which has been previously described, for example, for the influence of mechanical stimulation (Li et al., 2010). Indeed, within this group the donor variability was observable with gelMA embedded donor cells performing similar (Donor 1 P3) or slightly better (Donor 1 P5) than pellet culture or significantly worse (Donors 2 and 3). The differentiation effect of the two hydrogel stiffnesses was comparable.

Generally, in comparison to the gelMA groups, the pellet culture promoted increased chondrogenic differentiation, which might be related to the closer proximity of cells, influencing each other by paracrine (Grassel et al., 2010; Li et al., 2010; Takigawa et al., 1997) and cell-cell contact (Tsuchiya et al., 2004) stimulation, which have both been previously shown to stimulate differentiation. Despite that, donor variability was high and especially observable with the addition of low growth factor concentration. Differences were mainly found in the total increase in gene expression, but did not show differences between cultivation systems (gelMA vs. pellet culture). Passage number (P3 vs. P5) only marginally influenced the behavior of the chondrocytes within gelMA and pellet culture for both, low and high doses of growth factors. Chondrogenic differentiation was consistent

between P3 and P5, showing that also after expansion over the critical passage number of 5 (Kang et al., 2007) chondrocyte re-differentiation was possible, both in gelMA and in pellet culture. However, in the clinical setting, the appropriate growth factor condition might not be present, especially in inflammatory conditions such as OA. For such conditions co-embedding of growth factors or anti-inflammatory therapeutics, which has been previously achieved (Gnavi et al., 2014; Moshaverinia et al., 2015; Yamamoto et al., 1999), might be a successful strategy when using a gelMA hydrogel as a delivery system.

Another clinically relevant option for cartilage damage repair is the use of autologous MSC alone or in co-culture as they have a chondrogenic potential and can be more easily obtained, for example, from fat tissue. Likewise the amount of hAC needed for clinical interventions may be reduced, also enabling 1-step procedures, thereby alleviating the need for a second surgery. This aspect, in combination with an overall reduction in amount of cells (due to a direct application to the site of interest and alleviation of cell-loss of non-adhering cells when applied to the joint cavity in suspension), could greatly improve the treatment of diseases such as OA. Furthermore, as MSC are known to have immuno-modulatory effects, they might counteract inflammation, and therefore positively influence cartilage regeneration, in OA defects (van Buul et al., 2012). Additionally some studies suggest a positive effect on differentiation capacity in co-cultures between hAC and MSC (Dahlin et al., 2014; Hildner et al., 2009; Tsuchiya et al., 2004).

In OA non-cell based treatments such as hyaluronic acid (Bowman et al., 2018) or cell-based therapies (Burdick et al., 2016) are frequently applied by an intraarticular injection. This application has resulted in varying degrees of success which is likely caused by low amounts or transient availability of non-cellular therapeutics and/or cells reaching the region of defect, or being maintained there. It has been shown that for cell based therapy in many cases less than 5% of initially applied cells are retained at the site of injection (Burdick et al., 2016). The use of gelMA might alleviate these problems by keeping cells at the defect site, while protecting the cells and smoothening the joint surface, while still being applicable endoscopically, thereby preventing further damage. In this study this was tested using an osteochondral plug model (obtained from OA patients) and simulation of the strain during normal human gait using a tribometer. The results show that the hydrogel was stable on the underlying cartilage when mimicking the conditions within a healthy joint (coefficient of friction of 0.005 – 0.023) (Charnley, 1960), the cells were evenly distributed (mixture of hAC and ASC/TERT1) and remained viable under the applied mechanical stress.

5 | CONCLUSIONS

In conclusion, gelMA is a promising hydrogel for cartilage regeneration as it combines easy application of cells into defect areas and protection against harmful influences, while allowing for efficient (re-)differentiation of hAC. Due to its characteristics, it is possible to fill surface roughness or replace larger superficial tissue loss, for example, in OA defects, thereby making it a promising tool for the clinical treatment of OA.

5.1 | Limitations of the study

This study is limited by the high donor variability of primary human chondrocytes, which on the other hand is also advantageous, as it reflects the real clinical situation. The limited number of samples was due to limited donor availability and long cultivation time necessary to generate high passage chondrocytes (especially from older donors). Additionally, due to the low reproducibility of the measurements obtained with the available setup for mechanical testing, samples were therefore mainly analyzed for cell viability and intactness/attachment of the hydrogel.

CONFLICT OF INTEREST

The authors declare that there is no conflict of interest.

AUTHOR CONTRIBUTIONS

Writing the manuscript: Katja Hölzl, Marian Fürsatz. Isolation/culture of cells and tissue: Katja Hölzl, Marian Fürsatz, Sara Žigon-Branc, Marica Markovic. Cytotoxicity assays: Katja Hölzl, Rheology: Katja Hölzl, Stefan Baudis, Confocal Imaging: Katja Hölzl, Marian Fürsatz, qRT-PCR: Katja Hölzl, Histology: Barbara Schädl. Synthesis of gelMA: Jasper Van Hoorick, Sandra Van Vlierberghe. Mechanical testing: Hakan Göcerler, Andreas Pauschitz, Katja Hölzl. Statistical analysis: Claudia Gahleitner, Study design: Katja Hölzl, Aleksandr Ovsianikov, Heinz Redl, Sylvia Nürnberger. Data analysis and interpretation: Katja Hölzl, Marian Fürsatz, Hakan Göcerler, Sylvia Nürnberger. Critically reviewing the manuscript: all

DATA AVAILABILITY STATEMENT

The data that support the findings of this study are available from the corresponding author upon reasonable request.

ORCID

Marian Fürsatz https://orcid.org/0000-0003-4990-3326

REFERENCES

Akkiraju, H., & Nohe, A. (2015). Role of chondrocytes in cartilage formation, progression of osteoarthritis and cartilage regeneration. *Journal of Developmental Biology*, 3(4), 177–192. https://doi.org/10.3390/jdb3040177

Allen, J. L., Cooke, M. E., & Alliston, T. (2012). ECM stiffness primes the TGFβ pathway to promote chondrocyte differentiation. *Molecular Biology of the Cell*, 23(18), 3731–3742. https://doi.org/10.1091/mbc.e12-03-0172

Almeida, H. V., Eswaramoorthy, R., Cunniffe, G. M., Buckley, C. T., O'Brien, F. J., & Kelly, D. J. (2016). Fibrin hydrogels functionalized with cartilage extracellular matrix and incorporating freshly isolated stromal cells as an injectable for cartilage regeneration. *Acta Biomaterialia*, 36, 55–62. https://doi.org/10.1016/j.actbio.2016.03.008

Almqvist, K. F. (2001). Culture of chondrocytes in alginate surrounded by fibrin gel: Characteristics of the cells over a period of eight weeks. *Annals of the Rheumatic Diseases*, 60(8), 781–790. https://doi.org/10.1136/ard.60.8.781

Alves da Silva, M. L., Crawford, A., Mundy, J. M., Correlo, V. M., Sol, P., Bhattacharya, M., Hatton, P. V., Reis, R. L., & Neves, N. M. (2010). Chitosan/polyester-based scaffolds for cartilage tissue engineering: Assessment of extracellular matrix formation. *Acta Biomaterialia*, 6(3), 1149–1157. https://doi.org/10.1016/j.actbio.2009.09.006

Assmann, A., Vegh, A., Ghasemi-Rad, M., Bagherifard, S., Cheng, G., Sani, E. S., Ruiz-Esparza, G. U., Noshadi, I., Lassaletta, A. D., Gangadharan, S., Tamayol, A., Khademhosseini, A., & Annabi, N. (2017). A highly adhesive and naturally derived sealant. *Biomaterials*, 140, 115–127. https://doi.org/10.1016/j.biomaterials.2017.06.004

Bachmann, B., Spitz, S., Schädl, B., Teuschl, A. H., Redl, H., Nürnberger, S., & Ertl, P. (2020). Stiffness matters: Fine-tuned hydrogel elasticity alters chondrogenic redifferentiation. *Frontiers in Bioengineering and Biotechnology*, 8, 373. https://doi.org/10.3389/fbioe.2020.00373

Bhosale, A. M., & Richardson, J. B. (2008). Articular cartilage: Structure, injuries and review of management. *British Medical Bulletin*, 87, 77–95. https://doi.org/10.1093/bmb/ldn025

Bielli, A., Scioli, M. G., Gentile, P., Cervelli, V., & Orlandi, A. (2016). Adipose-derived stem cells in cartilage regeneration: Current perspectives. *Regenerative Medicine*, 11(7), 693–703. https://doi.org/10.2217/rme-2016-0077

Boere, K. W. M., Visser, J., Seyednejad, H., Rahimian, S., Gawlitta, D., van Steenbergen, M. J., Dhert, W. J. A., Hennink, W. E., Vermonden, T., & Malda, J. (2014). Covalent attachment of a three-dimensionally printed thermoplast to a gelatin hydrogel for mechanically enhanced cartilage constructs. *Acta Biomaterialia*, 10(6), 2602–2611. https://doi.org/10.1016/j.actbio.2014.02.041

Bowman, S., Awad, M. E., Hamrick, M. W., Hunter, M., & Fulzele, S. (2018). Recent advances in hyaluronic acid based therapy for osteoarthritis. *Clinical and Translational Medicine*, 7(1), 6. https://doi.org/10.1186/s40169-017-0180-3

Brittberg, M., Lindahl, A., Nilsson, A., Ohlsson, C., Isaksson, O., & Peterson, L. (1994). Treatment of deep cartilage defects in the knee with autologous chondrocyte transplantation. *New England Journal of Medicine*, 331(14), 889–895. https://doi.org/10.1056/NEJM199410063311401

Brown, G. C. J., Lim, K. S., Farrugia, B. L., Hooper, G. J., & Woodfield, T. B. F. (2017). Covalent incorporation of heparin improves chondrogenesis in photocurable gelatin-methacryloyl hydrogels. *Macromolecular Bioscience*, 17(12), 1700158. https://doi.org/10.1002/mabi.201700158

Burdick, J. A., Mauck, R. L., & Gerecht, S. (2016). To serve and protect: Hydrogels to improve stem cell-based therapies. *Cell Stem Cell*, 18(1), 13–15. https://doi.org/10.1016/j.stem.2015.12.004

Charnley, J. (1960). The lubrication of animal joints in relation to surgical reconstruction by arthroplasty. *Annals of the Rheumatic Diseases*, 19(1), 10–19. https://doi.org/10.1136/ard.19.1.10

Chen, X., Zhang, F., He, X., Xu, Y., Yang, Z., Chen, L., Zhou, S., Yang, Y., Zhou, Z., Sheng, W., & Zeng, Y. (2013). Chondrogenic differentiation of umbilical cord-derived mesenchymal stem cells in type I collagen-hydrogel for cartilage engineering. *Injury*, 44(4), 540–549. https://doi.org/10.1016/j.injury.2012.09.024

Dahlin, R. L., Ni, M., Meretoja, V. V., Kasper, F. K., & Mikos, A. G. (2014). TGF-β3-induced chondrogenesis in co-cultures of chondrocytes and mesenchymal stem cells on biodegradable scaffolds. *Biomaterials*, 35(1), 123–132. https://doi.org/10.1016/j.biomaterials.2013.09.086

Enea, D., Cecconi, S., Busilacchi, A., Manzotti, S., Gesuita, R., & Gigante, A. (2012). Matrix-induced autologous chondrocyte implantation (MACI) in the knee. *Knee Surgery, Sports Traumatology, Arthroscopy*, 20(5), 862–869. https://doi.org/10.1007/s00167-011-1639-1

Erickson, G. R., Gimble, J. M., Franklin, D. M., Rice, H. E., Awad, H., & Guilak, F. (2002). Chondrogenic potential of adipose tissue-derived stromal cells in vitro and in vivo. *Biochemical and Biophysical Research Communications*, 290(2), 763–769. https://doi.org/10.1006/bbrc.2001.6270

Fürsatz, M., Gerges, P., Wolbank, S., & Nürnberger, S. (2021). Autonomous spheroid formation by culture plate compartmentation. *Biofabrication*, 13(3), 035018. https://doi.org/10.1088/1758-5090/abe186

Garza, J. R., Campbell, R. E., Tjoumakaris, F. P., Freedman, K. B., Miller, L. S., Santa Maria, D., & Tucker, B. S. (2020). Clinical efficacy of intra-articular mesenchymal stromal cells for the treatment of knee osteoarthritis: A double-blinded prospective randomized controlled clinical trial. *The American Journal of Sports Medicine*, 48(3), 588–598. https://doi.org/10.1177/0363546519899923

Gnavi, S., di Blasio, L., Tonda-Turo, C., Mancardi, A., Primo, L., Ciardelli, G., Gambarotta, G., Geuna, S., & Perroteau, I. (2014). Gelatin-based hydrogel for vascular endothelial growth factor release in peripheral nerve tissue engineering: VEGF-releasing hydrogel. *Journal of Tissue Engineering and Regenerative Medicine*, 11(2), 459–470. https://doi.org/10.1002/term.1936

Gorsche, C., Harikrishna, R., Baudis, S., Knaack, P., Husar, B., Laeuger, J., Hoffmann, H., & Liska, R. (2017). Real time-NIR/MIR-photorheology: A versatile tool for the *in situ* characterization of photopolymerization reactions. *Analytical Chemistry*, 89(9), 4958–4968. https://doi.org/10.1021/acs.analchem.7b00272

Göçerler, H., Pfeil, B., Franek, F., Bauer, C., Niculescu-Morzsa, E., & Nehrer, S. (2019). The dominance of water on lubrication properties of articular joints. *Industrial Lubrication & Tribology*, 72(1), 31–37. https://doi.org/10.1108/ILT-02-2019-0064

Grassel, S., Rickert, M., Opolka, A., Bosserhoff, A., Angele, P., Grifka, J., & Anders, S. (2010). Coculture between periosteal explants and articular chondrocytes induces expression of TGF- 1 and collagen I. *Rheumatology*, 49(2), 218–230. https://doi.org/10.1093/rheumatology/kep326

Gu, L., Li, T., Song, X., Yang, X., Li, S., Chen, L., Liu, P., Gong, X., Chen, C., & Sun, L. (2020). Preparation and characterization of methacrylated gelatin/bacterial cellulose composite hydrogels for cartilage tissue engineering. *Regenerative Biomaterials*, 7(2), 195–202. https://doi.org/10.1093/rb/rbz050

Han, L., Xu, J., Lu, X., Gan, D., Wang, Z., Wang, K., Zhang, H., Yuan, H., & Weng, J. (2017). Biohybrid methacrylated gelatin/polyacrylamide hydrogels for cartilage repair. *Journal of Materials Chemistry B*, 5(4), 731–741. https://doi.org/10.1039/C6TB02348G

Han, M.-E., Kang, B. J., Kim, S.-H., Kim, H. D., & Hwang, N. S. (2017). Gelatin-based extracellular matrix cryogels for cartilage tissue engineering. *Journal of Industrial and Engineering Chemistry*, 45, 421–429. https://doi.org/10.1016/j.jiec.2016.10.011

Häuselmann, H. J., Masuda, K., Hunziker, E. B., Neidhart, M., Mok, S. S., Michel, B. A., & Thonar, E. J. (1996). Adult human chondrocytes cultured in alginate form a matrix similar to native human articular cartilage. *American Journal of Physiology*, 271(3 Pt 1), C742–C752. https://doi.org/10.1152/ajpcell.1996.271.3.C742

Hildner, F., Concaro, S., Peterbauer, A., Wolbank, S., Danzer, M., Lindahl, A., Gatenholm, P., Redl, H., & van Griensven, M. (2009). Human adipose-derived stem cells contribute to chondrogenesis in coculture with human articular chondrocytes. *Tissue Engineering Part A*, *15*(12), 3961–3969. https://doi.org/10.1089/ten.tea.2009.0002

Hunziker, E. B., Lippuner, K., Keel, M. J. B., & Shintani, N. (2015). An educational review of cartilage repair: Precepts & practice--myths & misconceptions--progress & prospects. *Osteoarthritis and Cartilage*, *23*(3), 334–350. https://doi.org/10.1016/j.joca.2014.12.011

Kang, S.-W., Yoo, S. P., & Kim, B.-S. (2007). Effect of chondrocyte passage number on histological aspects of tissue-engineered cartilage. *Bio-Medical Materials and Engineering*, *17*(5), 269–276.

Knezevic, L., Schaupper, M., Mühleder, S., Schimek, K., Hasenberg, T., Marx, U., Priglinger, E., Redl, H., & Holnthoner, W. (2017). Engineering blood and lymphatic microvascular networks in fibrin matrices. *Frontiers in Bioengineering and Biotechnology*, *5*. https://doi.org/10.3389/fbioe.2017.00025

Koh, R. H., Jin, Y., Kim, J., & Hwang, N. S. (2020). Inflammation-modulating hydrogels for osteoarthritis cartilage tissue engineering. *Cells*, *9*(2), 419. https://doi.org/10.3390/cells9020419

Lee, D. A., Reisler, T., & Bader, D. L. (2003). Expansion of chondrocytes for tissue engineering in alginate beads enhances chondrocytic phenotype compared to conventional monolayer techniques. *Acta Orthopaedica Scandinavica*, *74*(1), 6–15. https://doi.org/10.1080/000164 70310013581

Li, X., Chen, S., Li, J., Wang, X., Zhang, J., Kawazoe, N., & Chen, G. (2016). 3D culture of chondrocytes in gelatin hydrogels with different stiffness. *Polymers*, *8*(8), 269. https://doi.org/10.3390/polym8080269

Li, Z., Kupcsik, L., Yao, S.-J., Alini, M., & Stoddart, M. J. (2010). Mechanical load modulates chondrogenesis of human mesenchymal stem cells through the TGF-β pathway. *Journal of Cellular and Molecular Medicine*, *14*(6a), 1338–1346. https://doi.org/10.1111/j.1582-4934.2009.00780.x

Liu, M., Zeng, X., Ma, C., Yi, H., Ali, Z., Mou, X., Li, S., Deng, Y., & He, N. (2017). Injectable hydrogels for cartilage and bone tissue engineering. *Bone Research*, *5*, 17014. https://doi.org/10.1038/boneres.2017.14

Majima, T., Schnabel, W., & Weber, W. (1991). Phenyl-2,4,6-trimethylbenzoylphosphinates as water-soluble photoinitiators. Generation and reactivity of O=b(C6Hs)(O-) radical anions. *Makromolekulare Chemie*, *192*(10), 2307–2315. https://doi.org/10.1002/macp.1991.021921010

Markovic, M., Van Hoorick, J., Hölzl, K., Tromayer, M., Gruber, P., Nürnberger, S., Dubruel, P., Van Vlierberghe, S., Liska, R., & Ovsianikov, A. (2015). Hybrid tissue engineering scaffolds by combination of three-dimensional printing and cell photoencapsulation. *Journal of Nanotechnology in Engineering and Medicine*, *6*(2), 021001. https://doi.org/10.1115/1.4031466

Migliorini, F., Rath, B., Colarossi, G., Driessen, A., Tingart, M., Niewiera, M., & Eschweiler, J. (2020). Improved outcomes after mesenchymal stem cells injections for knee osteoarthritis: Results at 12-months follow-up: A systematic review of the literature. *Archives of Orthopaedic and Trauma Surgery*, *140*(7), 853–868. https://doi.org/10.1007/s00402-019-03267-8

Moshaverinia, A., Chen, C., Xu, X., Ansari, S., Zadeh, H. H., Schricker, S. R., Paine, M. L., Moradian-Oldak, J., Khademhosseini, A., Snead, M. L., & Shi, S. (2015). Regulation of the stem cell-host immune system interplay using hydrogel coencapsulation system with an anti-inflammatory drug. *Advanced Functional Materials*, *25*(15), 2296–2307. https://doi.org/10.1002/adfm.201500055

Mouser, V. (2018). Ex vivo model unravelling cell distribution effect in hydrogels for cartilage repair. *ALTEX*, *35*(1), 65–76. https://doi.org/10.14573/altex.1704171

Muñoz-Criado, I., Meseguer-Ripolles, J., Mellado-López, M., Alastrue-Agudo, A., Griffeth, R. J., Forteza-Vila, J., Cugat, R., García, M., &

Moreno-Manzano, V. (2017). Human suprapatellar fat pad-derived mesenchymal stem cells induce chondrogenesis and cartilage repair in a model of severe osteoarthritis. *Stem Cells International*, *2017*, 1–12. https://doi.org/10.1155/2017/4758930

Nürnberger, S., Schneider, C., van Osch, G. V. M., Keibl, C., Rieder, B., Monforte, X., Teuschl, A. H., Mühleder, S., Holnthoner, W., Schädl, B., Gahleitner, C., Redl, H., & Wolbank, S. (2019). Repopulation of an auricular cartilage scaffold, AuriScaff, perforated with an enzyme combination. *Acta Biomaterialia*, *86*, 207–222. https://doi.org/10.1016/j.actbio.2018.12.035

Ovsianikov, A., Deiwick, A., Van Vlierberghe, S., Dubruel, P., Möller, L., Dräger, G., & Chichkov, B. (2011). Laser fabrication of three-dimensional CAD scaffolds from photosensitive gelatin for applications in tissue engineering. *Biomacromolecules*, *12*(4), 851–858. https://doi.org/10.1021/bm1015305

Park, H., & Lee, K. Y. (2014). Cartilage regeneration using biodegradable oxidized alginate/hyaluronate hydrogels: Cartilage regeneration using biodegradable hydrogels. *Journal of Biomedical Materials Research Part A*, *102*(12), 4519–4525. https://doi.org/10.1002/jbm.a.35126

Patil, S., Steklov, N., Song, L., Bae, W. C., & D'Lima, D. D. (2014). Comparative biomechanical analysis of human and caprine knee articular cartilage. *The Knee*, *21*(1), 119–125. https://doi.org/10.1016/j.knee.2013.03.009

Perka, C., Schultz, O., Lindenhayn, K., Spitzer, R. S., Muschik, M., Sittinger, M., & Burmester, G. R. (2000). Joint cartilage repair with transplantation of embryonic chondrocytes embedded in collagen-fibrin matrices. *Clinical & Experimental Rheumatology*, *18*(1), 13–22.

Salam, N., Toumpaniari, S., Gentile, P., Marina Ferreira, A., Dalgarno, K., & Partridge, S. (2018). Assessment of migration of human MSCs through fibrin hydrogels as a tool for formulation optimisation. *Materials*, *11*(9), 1781. https://doi.org/10.3390/ma11091781

Song, Y., Du, H., Dai, C., Zhang, L., Li, S., Hunter, D. J., Lu, L., & Bao, C. (2018). Human adipose-derived mesenchymal stem cells for osteoarthritis: A pilot study with long-term follow-up and repeated injections. *Regenerative Medicine*, *13*(3), 295–307. https://doi.org/10.2217/rme-2017-0152

Sophia Fox, A. J., Bedi, A., & Rodeo, S. A. (2009). The basic science of articular cartilage. *Sport Health*, *1*(6), 461–468. https://doi.org/10.1177/1941738109350438

Takigawa, M., Okawa, T., Pan, H.-O., Aoki, C., Takahashi, K., Zue, J.-D., Suzuki, F., & Kinoshita, A. (1997). Insulin-like growth factors I and II are autocrine factors in stimulating proteoglycan synthesis, a marker of differentiated chondrocytes, acting through their respective receptors on a clonal human chondrosarcoma-derived chondrocyte cell line. *Endocrinology*, *138*(10), 11.

Toupet, K., Maumus, M., Peyrafitte, J.-A., Bourin, P., van Lent, P. L. E. M., Ferreira, R., Orsetti, B., Pirot, N., Casteilla, L., Jorgensen, C., & Noël, D. (2013). Long-term detection of human adipose-derived mesenchymal stem cells after intraarticular injection in SCID mice: Biodistribution and long-term detection of human AD-MSCs in SCID mice. *Arthritis & Rheumatism*, *65*(7), 1786–1794. https://doi.org/10.1002/art.37960

Tsuchiya, K., Chen, G., Ushida, T., Matsuno, T., & Tateishi, T. (2004). The effect of coculture of chondrocytes with mesenchymal stem cells on their cartilaginous phenotype in vitro. *Materials Science and Engineering: C*, *24*(3), 391–396. https://doi.org/10.1016/j.msec.2003.12.014

van Buul, G. M., Villafuertes, E., Bos, P. K., Waarsing, J. H., Kops, N., Narcisi, R., Weinans, H., Verhaar, J. a. N., Bernsen, M. R., & van Osch, G. J. V. M. (2012). Mesenchymal stem cells secrete factors that inhibit inflammatory processes in short-term osteoarthritic synovium and cartilage explant culture. *Osteoarthritis and Cartilage*, *20*(10), 1186–1196. https://doi.org/10.1016/j.joca.2012.06.003

Van Den Bulcke, A. I., Bogdanov, B., De Rooze, N., Schacht, E. H., Cornelissen, M., & Berghmans, H. (2000). Structural and rheological

properties of methacrylamide modified gelatin hydrogels. *Biomacromolecules*, 1(1), 31–38. https://doi.org/10.1021/bm990017d

Van Hoorick, J., Declercq, H., De Muynck, A., Houben, A., Van Hoorebeke, L., Cornelissen, R., Van Erps, J., Thienpont, H., Dubruel, P., & Van Vlierberghe, S. (2015). Indirect additive manufacturing as an elegant tool for the production of self-supporting low density gelatin scaffolds. *Journal of Materials Science: Materials in Medicine*, 26(10), 247. https://doi.org/10.1007/s10856-015-5566-4

Van Hoorick, J., Gruber, P., Markovic, M., Rollot, M., Graulus, G.-J., Vagenende, M., Tromayer, M., Van Erps, J., Thienpont, H., Martins, J. C., Baudis, S., Ovsianikov, A., Dubruel, P., & Van Vlierberghe, S. (2018). Highly reactive thiol-norbornene photo-click hydrogels: Toward improved processability. *Macromolecular Rapid Communications*, 39(14), 1800181. https://doi.org/10.1002/marc.201800181

Van Hoorick, J., Tytgat, L., Dobos, A., Ottevaere, H., Van Erps, J., Thienpont, H., Ovsianikov, A., Dubruel, P., & Van Vlierberghe, S. (2019). (Photo-)crosslinkable gelatin derivatives for biofabrication applications. *Acta Biomaterialia*, 97, 46–73. https://doi.org/10.1016/j.actbio.2019.07.035

Wang, K.-Y., Jin, X.-Y., Ma, Y.-H., Cai, W.-J., Xiao, W.-Y., Li, Z.-W., Qi, X., & Ding, J. (2021). Injectable stress relaxation gelatin-based hydrogels with positive surface charge for adsorption of aggrecan and facile cartilage tissue regeneration. *Journal of Nanobiotechnology*, 19(1), 214. https://doi.org/10.1186/s12951-021-00950-0

Wei, W., Ma, Y., Yao, X., Zhou, W., Wang, X., Li, C., Lin, J., He, Q., Leptihn, S., & Ouyang, H. (2021). Advanced hydrogels for the repair of cartilage defects and regeneration. *Bioactive Materials*, 6(4), 998–1011. https://doi.org/10.1016/j.bioactmat.2020.09.030

Wolbank, S., Pichler, V., Ferguson, J. C., Meinl, A., van Griensven, M., Goppelt, A., & Redl, H. (2015). Non-invasive *in vivo* tracking of fibrin degradation by fluorescence imaging: *In vivo* imaging of fibrin degradation. *Journal of Tissue Engineering and Regenerative Medicine*, 9(8), 973–976. https://doi.org/10.1002/term.1941

Yamamoto, M., Tabata, Y., & Ikada, Y. (1999). Growth factor release from gelatin hydrogel for tissue engineering. *Journal of Bioactive and Compatible Polymers*, 14(6), 474–489. https://doi.org/10.1177/088391159901400603

Yoon, J., Ha, S., Lee, S., & Chae, S.-W. (2018). Analysis of contact pressure at knee cartilage during gait with respect to foot progression angle. *International Journal of Precision Engineering and Manufacturing*, 19(5), 761–766. https://doi.org/10.1007/s12541-018-0091-2

Yue, K., Li, X., Schrobback, K., Sheikhi, A., Annabi, N., Leijten, J., Zhang, W., Zhang, Y. S., Hutmacher, D. W., Klein, T. J., & Khademhosseini, A. (2017). Structural analysis of photocrosslinkable methacryloyl-modified protein derivatives. *Biomaterials*, 139, 163–171. https://doi.org/10.1016/j.biomaterials.2017.04.050

Zhang, L., Hu, J., & Athanasiou, K. A. (2009). The role of tissue engineering in articular cartilage repair and regeneration. *Critical Reviews in Biomedical Engineering*, 37(1–2), 1–57.

Zhou, F., Hong, Y., Zhang, X., Yang, L., Li, J., Jiang, D., Bunpetch, V., Hu, Y., Ouyang, H., & Zhang, S. (2018). Tough hydrogel with enhanced tissue integration and in situ forming capability for osteochondral defect repair. *Applied Materials Today*, 13, 32–44. https://doi.org/10.1016/j.apmt.2018.08.005

Žigon-Branc, S., Markovic, M., Van Hoorick, J., Van Vlierberghe, S., Dubruel, P., Zerobin, E., Baudis, S., & Ovsianikov, A. (2019). Impact of hydrogel stiffness on differentiation of human adipose-derived stem cell microspheroids. *Tissue Engineering Part A*, 25(19–20), 1369–1380. https://doi.org/10.1089/ten.tea.2018.0237

SUPPORTING INFORMATION

Additional supporting information may be found in the online version of the article at the publisher's website.

How to cite this article: Hölzl, K., Fürsatz, M., Göcerler, H., Schädl, B., Žigon-Branc, S., Markovic, M., Gahleitner, C., Hoorick, J. V., Van Vlierberghe, S., Kleiner, A., Baudis, S., Pauschitz, A., Redl, H., Ovsianikov, A., & Nürnberger, S. (2022). Gelatin methacryloyl as environment for chondrocytes and cell delivery to superficial cartilage defects. *Journal of Tissue Engineering and Regenerative Medicine*, 16(2), 207–222. https://doi.org/10.1002/term.3273